The Canadian Mineralogist
Vol. 54, pp. 1087-1101 (2016)
DOI: 10.3749/canmin.1600033

CRYSTAL CHEMISTRY OF THE WYLLIEITE GROUP OF PHOSPHATE MINERALS

FRÉDÉRIC HATERT[§]

Laboratoire de Minéralogie, B18, Université de Liège, B-4000 Sart-Tilman, Belgium

MIGUEL GALLISKI

IANIGLA-CONICET, C.C. 330 Avda. A. Ruiz Leal s/n, Parque Gral. San Martin, 5500 Mendoza, Argentina

ENCARNACIÓN RODA-ROBLES

Dpto. Mineralogía y Petrología, Universidad del País Vasco/EHU, Apdo. 644, E-48080 Bilbao, Spain

PIETRO VIGNOLA

CNR-Istituto per la Dinamica dei Processi Ambientali, via Mario Bianco, 9, I-20131 Milano, Italy

ANDRÉ-MATHIEU FRANSOLET

Laboratoire de Minéralogie, B18, Université de Liège, B-4000 Sart-Tilman, Belgium

ABSTRACT

Three samples of minerals belonging to the wyllieite mineral group were structurally investigated: wyllieite from the Buranga pegmatite, Rwanda (A); wyllieite from the Malpensata pegmatite, Italy (B); and qingheiite from the Santa Ana pegmatite, Argentina (C). Their crystal structures were refined, based on single-crystal X-ray diffraction data, to $R_1 = 2.72\%$ (A), 3.53% (B), and 2.46% (C). Unit-cell parameters are: *a* 11.954(2), *b* 12.439(2), *c* 6.406(1) Å, β 114.54(1)° (A); *a* 11.983(1), *b* 12.423(1), *c* 6.381(1) Å, β = 114.54(1)° (B); *a* 11.878(3), *b* 12.448(2), *c* 6.438(2) Å, β 114.49(1)° (C). The structure consists of kinked chains of edge-sharing octahedra stacked parallel to {101}. These chains are formed by a succession of M(2a)–M(2b) octahedral pairs, linked by slightly larger M(1) octahedra. Equivalent chains are connected in the *b* direction by the P(1), P(2a), and P(2b) phosphate tetrahedra to form sheets oriented perpendicular to [010]. These interconnected sheets produce channels parallel to **c**, channels that contain the large X cations. The X(1a) site is coordinated by anions in a distorted octahedral coordination, whereas the X(1b) site coordination can be described as a very distorted cube. The morphology of the X(2) coordination corresponds to a very distorted gable disphenoid with a [7 + 1] coordination, similar to the coordination of the A(2)' site in the alluaudite structure. The structural features of these phosphate minerals are compared to those of other wyllieite-type phosphates: ferrorosemaryite, rosemaryite, and qingheiite-(Fe^{2+}). These new structural data indicate that Al is predominant at the M(2a) site in the investigated samples, with Fe^{2+}, Fe^{3+}, or Mg at the M(2b) site. Variations of unit-cell parameters, of bond distances, and of distortion coefficients among members of the wyllieite group are discussed in detail.

Keywords: phosphate minerals, wyllieite group, crystal structure, oxidation mechanisms.

INTRODUCTION

The wyllieite group of minerals contains Na-Mn-Fe-Mg-Al-bearing phosphates which occur in rare-element granitic pegmatites, particularly in the beryl-columbite-phosphate and spodumene subtypes, according to the classification of Černý (1991) and Černý & Ercit (2005). Moore & Molin-Case (1974) solved the crystal structure of ferrowyllieite, $Na_2Fe^{2+}{}_2Al(PO_4)_3$, and showed that it is topologically identical to the alluaudite structure (Moore 1971). However, the ordering of

[§] *Corresponding author e-mail address*: fhatert@ulg.ac.be

cations in ferrowyllieite induces a splitting of the M(2) and X(1) sites of alluaudite into the M(2a)-M(2b) and X(1a)-X(1b) sites, with a concurrent change of space group from $C2/c$ to $P2_1/n$. The structural formula of the wyllieite-type phosphate minerals then becomes $X(2)X(1a)_{0.5}X(1b)_{0.5}M(1)M(2a)M(2b)(PO_4)_3$ (Moore & Molin-Case 1974).

The crystal chemistry of these phosphates was investigated by Moore & Ito (1979), who proposed a revision of their nomenclature based on chemical data. According to these authors, the name wyllieite corresponds to $Na_2MnFe^{2+}Al(PO_4)_3$, whereas the name rosemaryite designates the more oxidized composition $NaMnFe^{3+}Al(PO_4)_3$. The prefix ferro- is then added if Fe^{2+} dominates at the M(1) site, thus leading to ferrowyllieite (Moore & Ito 1973) or ferrorosemaryite (Hatert *et al*. 2005). The name qingheiite was introduced by Zhesheng *et al*. (1983) for the Mg-rich equivalent of wyllieite, $Na_2MnMgAl(PO_4)_3$.

A structural study of the new mineral species ferrorosemaryite, $NaFe^{2+}Fe^{3+}Al(PO_4)_3$, revealed that it belongs to the wyllieite group of minerals, with Al prevailing at the M(2a) site (Hatert *et al*. 2005). This unexpected cation distribution, different from that observed in ferrowyllieite by Moore & Molin-Case (1974), was confirmed in rosemaryite from the Buranga pegmatite, Rwanda (Hatert *et al*. 2006), as well as in the recently described species qingheiite-(Fe^{2+}), $Na_2Fe^{2+}MgAl(PO_4)_3$ (Hatert *et al*. 2010).

To date, wyllieite is the only species in the wyllieite group which has never been structurally investigated. In this paper, we consequently present a structural study of wyllieite from the Buranga pegmatite, Rwanda, of wyllieite from the Malpensata pegmatite, Italy, and of qingheiite from the Santa Ana pegmatite, Argentina. A petrographic study of ferrowyllieite and ferrorosemaryite from a pegmatite of the Albères Massif, France, will finally help us to shed some light on the oxidation mechanisms responsible for the transition between these two phosphate minerals.

Analytical Methods

Electron-microprobe compositions of ferrowyllieite and ferrorosemaryite from the Albères Massif (Table 1) were obtained with a Cameca SX-50 instrument located in Toulouse, France (analyst P. de Parseval), which was operated in the wavelength-dispersion mode. Accelerating voltage and beam current were 15 kV and 20 nA, with a spot size of 5 μm, and a counting time of 30 s on the peaks and 10 s on the background. The standards used were graftonite from Sidi-bou-Othmane (P, Mn), corundum (Al), hematite (Fe), periclase (Mg), rhodonite (Zn), wollastonite (Ca), sanidine (K), and albite (Na). Compositions of wyllieite from the Malpensata pegmatite (Table 1) were collected with a JEOL JXA-8200 electron microprobe, working in wavelength-dispersion mode, at the Department of Earth Sciences, University of Milan. The system was operated with an accelerating voltage of 15 kV, a beam current of 5 nA, a spot size of 5 μm, and a counting time of 30 s on the peaks and 10 s on the background. The following natural minerals were used as standards: graftonite KF16 (Fransolet 1975; P, Fe, Mn, Ca), anorthite-An137 (Al), olivine-USNM2566 (Mg), omphacite-USNM110607 (Na), and orthoclase-PSU OR1A (K). The raw data were corrected for matrix effects using the φρZ method from the JEOL series of programs.

The X-ray structural investigation of wyllieite from Buranga and of qingheiite were carried out with a Bruker $P4$ four-circle diffractometer (Mo$K\alpha$ radiation, $\lambda = 0.71073$ Å), using crystal fragments with dimensions $0.07 \times 0.08 \times 0.12$ mm (wyllieite) and $0.55 \times 0.40 \times 0.32$ (qingheiite) mm. The unit-cell parameters and standard deviations were calculated for the setting angles of 29 [wyllieite: a 11.954(2), b 12.439(2), c 6.406(1) Å, and β 114.54(1)°] and 25 reflections [qingheiite: a 11.878(3), b 12.448(2), c 6.438(2) Å, and β 114.49(1)°]. The intensities of 2759 (wyllieite) and 2749 (qingheiite) reflections, corresponding to 2003 (wyllieite) and 1997 (qingheiite) unique reflections, were measured by the ω scan technique. Data were corrected for Lorentz, polarization and absorption effects, the latter with a semi-empirical method using a reliable set of ψ-scan data. The X-ray structural study of wyllieite from Malpensata was carried out with an Agilent Technologies Excalibur 4-circle diffractometer equipped with an EOS CCD-area detector, on a crystal fragment measuring $0.06 \times 0.13 \times 0.28$ mm. Some 217 frames with a spatial resolution of 1° were collected by the φ/ω scan technique, with a counting time of 10 s per frame, in the range $4.96 < 2\theta < 57.36°$. A total of 3781 reflections were extracted from these frames, corresponding to 1971 unique reflections; the refined unit-cell parameters are a 11.983(1), b 12.423(1), c 6.381(1) Å, and β 114.54(1)°. Data were corrected for Lorentz, polarization and absorption effects, the latter with an analytical method using the SCALE3 ABSPACK scaling algorithm included in the CrysAlisRED package (Oxford Diffraction 2007). More details on data collection, reduction, and structure refinement procedures are given in Table 2.

Infrared spectra (Fig. 1) were recorded with a Nicolet NEXUS spectrometer, from 32 scans with a 1 cm^{-1} resolution, over the 400–4000 cm^{-1} region. The sample was prepared by intimately mixing 2 mg of

TABLE 1. CHEMICAL ANALYSES OF WYLLIEITE-TYPE PHOSPHATES

	1	2	3	4	5	6	7
P_2O_5	44.44	42.87	42.99	44.19	44.00	44.35	44.36
Al_2O_3	7.78	7.00	7.56	7.39	6.68	7.32	5.13
Fe_2O_3	3.46	0.00	0.00	1.11	9.22	0.79	3.99
FeO	11.96	22.96	22.92	22.75	16.21	22.63	6.07
MnO	19.16	14.38	13.96	15.43	13.74	16.71	21.48
MgO	1.70	2.00	1.90	1.99	1.91	0.23	8.07
ZnO	-	0.22	0.00	0.06	0.00	-	0.00
CaO	0.42	0.80	0.79	0.44	0.74	0.77	0.58
Na_2O	9.86	8.60	7.68	6.36	4.98	8.49	9.57
K_2O	0.04	0.01	0.04	0.11	0.01	0.01	0.01
Total	98.82	98.84	97.84	99.83	97.49	101.30	99.26
Cation numbers							
P	3.000	3.000	3.000	3.000	3.000	3.000	3.000
Al	0.731	0.682	0.734	0.698	0.634	0.690	0.483
Fe^{3+}	0.208	0.000	0.000	0.067	0.559	0.048	0.240
Fe^{2+}	0.797	1.588	1.580	1.526	1.092	1.512	0.406
Mn^{2+}	1.294	1.007	0.975	1.048	0.937	1.131	1.453
Mg	0.201	0.246	0.233	0.238	0.229	0.028	0.960
Zn	-	0.013	0.000	0.004	0.000	-	0.000
Ca	0.035	0.071	0.069	0.037	0.064	0.066	0.050
Na	1.524	1.378	1.227	0.989	0.777	1.315	1.482
K	0.004	0.001	0.004	0.011	0.001	0.001	0.001
Sum	4.794	4.986	4.822	4.618	4.293	4.791	5.075

Note: Cation numbers were calculated on the basis of 3 P atoms per formula unit. The Fe^{2+}/Fe^{3+} ratio was calculated to maintain charge balance.

1. Wyllieite, Buranga, Rwanda. Sample Bu 5.5, Fransolet (1995), Average of two wet-chemical analyses. 2. Ferrowyllieite, Albères Massif. Sample AM48F, average of 6 point analyses. 3. Ferrowyllieite, Albères Massif. Sample AM48D, average of 11 point analyses. 4. Ferrowyllieite, Albères Massif. Sample TRIF1, average of 10 point analyses. 5. Ferrorosemaryite, Albères Massif. Sample AM48D, average of 3 point analyses. 6. Wyllieite, Malpensata pegmatite, Italy. Average of 60 point analyses. 7. Qingheiite, Santa Ana, Argentina. Sample SA07V, average of three electron-microprobe analyses performed under the same experimental conditions as those reported by Galliski *et al.* (2009).

sample with KBr in order to obtain a 150 mg homogeneous pellet which was subsequently dried for a few hours at 110 °C. To prevent water contamination, the measurements were performed using a purge of dry air.

Sample Selection and Description

The wyllieite sample from the Buranga pegmatite, Rwanda (no. Bu 5.5) is the same as that described earlier by Fransolet (1995). The wet-chemical analysis of this sample is given in Table 1; the resulting structural formula is $Na_{0.790}(Na_{0.734}Mn_{0.231}Ca_{0.035})_{\Sigma 1.00}(Mn)_{\Sigma 1.00}(Fe^{2+}_{0.797}Fe^{3+}_{0.140}Mn_{0.063})(Al_{0.731}Mg_{0.201}Fe^{3+}_{0.068})_{\Sigma 1.00}(PO_4)_3$. The unit-cell parameters, calculated from the X-ray powder diffraction pattern, are *a* 11.967(2), *b* 12.462(3), *c* 6.409(1) Å, and β 114.63(2)° (Fransolet 1995). The primitive space group of wyllieite from Buranga was confirmed by Fransolet (1995) from Weissenberg data, thus eliminating the possibility of the *C*-centered alluaudite space group.

The wyllieite sample from the Malpensata albite pegmatite was collected by P. Vignola (Vignola *et al.* 2011; PV collection catalogue no. 1684); it forms large massive dark green masses (behaving as single crystals under polarizing light) reaching 25 cm in diameter and showing a well-evident cleavage, included in a matrix of albite, quartz, and muscovite (Fig. 2a). Electron-microprobe analyses (Table 1) indicate an empirical formula of $Na_{0.790}(Na_{0.525}Mn_{0.409}Ca_{0.066})_{\Sigma 1.00}(Mn_{0.722}Fe^{2+}_{0.278})_{\Sigma 1.00}(Fe^{2+})(Al_{0.690}Mg_{0.028}Fe^{3+}_{0.048}Fe^{2+}_{0.234})_{\Sigma 1.00}(PO_4)_3$.

The qingheiite sample (no. SA07V, Miguel Galliski collection) was collected from the dumps of the Santa Ana pegmatite, Argentina. New electron-microprobe compositions (Table 1) indicate that this sample has an MgO content of up to 8.07 wt.%, whereas the samples from the same pegmatite investigated by Galliski *et al.*

TABLE 2. EXPERIMENTAL DETAILS FOR THE SINGLE-CRYSTAL X-RAY DIFFRACTION STUDY OF WYLLIEITE FROM BURANGA, OF WYLLIEITE FROM MALPENSATA, AND OF QINGHEIITE FROM SANTA ANA

	Wyllieite, Buranga	Wyllieite, Malpensata	Qingheiite, Santa Ana
Crystal dimensions (mm)	0.07 × 0.08 × 0.12	0.06 × 0.13 × 0.28	0.55 × 0.40 × 0.32
a (Å)	11.954(2)	11.983(1)	11.878(3)
b (Å)	12.439(2)	12.423(1)	12.448(2)
c (Å)	6.406(1)	6.381(1)	6.438(2)
β (°)	114.54(1)	114.54(1)	114.49(1)
Space group	$P2_1/n$	$P2_1/n$	$P2_1/n$
Z	4	4	4
Diffractometer	Bruker P4	Agilent Xcalibur, EOS CCD detector	Bruker P4
Operating conditions	50 kV, 30 mA	40 kV, 40 mA	50 kV, 30 mA
Radiation	Mo*K*α (λ = 0.71073 Å)	Mo*K*α (λ = 0.71073 Å)	Mo*K*α (λ = 0.71073 Å)
Scan mode	ω scan	φ/ω scan	ω scan
$2\theta_{min.}$, $2\theta_{max}$	4.98°, 55.00°	4.98°, 57.36°	5.00°, 54.98°
Range of indices	$-1 \le h \le 8$ $-16 \le k \le 1$ $-14 \le l \le 14$	$-16 \le h \le 13$ $-15 \le k \le 16$ $-6 \le l \le 8$	$-1 \le h \le 8$ $-1 \le k \le 16$ $-14 \le l \le 14$
Measured intensities	2759	3781	2749
Unique reflections	2003	1971	1997
Independent non-zero [$I > 2\sigma(I)$] reflections	1771	1735	1948
Absorption correction	Semi-empirical	Analytical numeric (crystal model)	Semi-empirical
μ (mm^{-1})	3.966	3.146	3.199
Data reduction program	SHELXTL-Plus (Sheldrick 1993)	CrysAlisPro (Oxford Diffraction 2007)	SHELXTL-Plus (Sheldrick 1993)
l.s. refinement program	SHELXL-93 (Sheldrick 2008)	SHELXL-93 (Sheldrick 2008)	SHELXL-93 (Sheldrick 2008)
Refined parameters	193	190	193
R_1 ($F_o > 2\sigma(F_o)$)	0.0272	0.0353	0.0246
R_1 (all)	0.0320	0.0418	0.0250
wR_2 (all)	0.0769	0.0989	0.0794
S (goodness of fit)	1.027	1.765	1.147
Max Δ/σ in the last l.s. cycle	0.001	0.000	0.000
Max peak and hole in the final Δ*F* map (*e*/Å^3)	+0.65 and –0.65	+0.63 and –0.53	+0.51 and –0.46

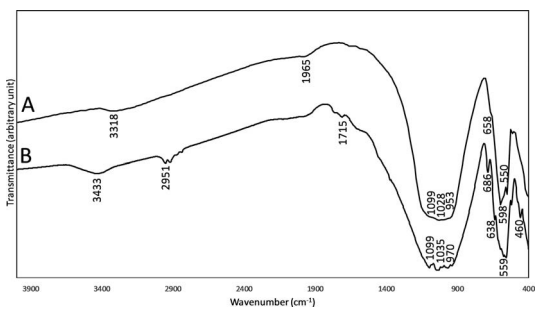

FIG. 1. Infrared spectra of wyllieite from Malpensata (A), and of qingheiite from Santa Ana (B).

(2009) have lower MgO contents of 4.08 and 6.21 wt.%. The resulting structural formula is $Na_{1.074}(Na_{0.408}Mn_{0.542}Ca_{0.050})_{\Sigma 1.00}(Mn_{0.911}Fe^{2+}_{0.089})_{\Sigma 1.00}(Al_{0.443}Fe^{3+}_{0.240}Fe^{2+}_{0.317})_{\Sigma 1.00}(Mg_{0.960}Al_{0.040})_{\Sigma 1.00}(PO_4)_3$.

The samples containing ferrowyllieite and ferrorosemaryite were collected by J.-C. Melgarejo and F. Fontan (†) from the Albères Massif, France. These phosphate minerals occur as irregular crystals associated with triphylite from type III pegmatites, as described by Malló *et al*. (1995). A petrographic examination of thin sections with a polarizing microscope showed that the colorless grains of ferrowyllieite are transformed, along fractures and on their rims, to greenish ferrorosemaryite (Fig. 2b). The chemical composition of

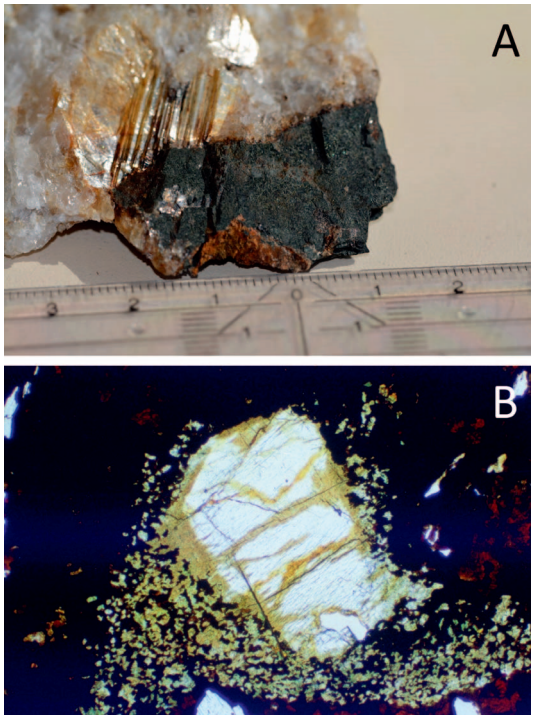

FIG. 2. (a) Dark green part of the wyllieite crystal from Malpensata, included in a matrix of quartz and muscovite. (b) Colorless grain of ferrowyllieite from the Albères Massif, included in black Fe-Mn-oxides. The ferrowyllieite grain is oxidized, along fractures and on its rim, to greenish ferrorosemaryite. Sample AM48D, plane-polarized light, length of the photograph 250 μm.

samples investigated by Malló *et al.* (1995) corresponds to Fe-rich wyllieite: $Na_{0.871}(Na_{0.592}Mn_{0.356}Ca_{0.052})_{\Sigma 1.00}(Mn_{0.511}Fe^{2+}_{0.489})_{\Sigma 1.00}(Fe^{2+})(Al_{0.718}Mg_{0.247}Fe^{2+}_{0.032}Zn_{0.003})_{\Sigma 1.00}(PO_4)_3$. However, the new electron-microprobe compositions of the samples investigated herein correspond to ferrowyllieite and ferrorosemaryite, since the M(1) site is dominantly occupied by Fe^{2+} (Table 1): $Na_{0.818}(Na_{0.409}Mn_{0.522}Ca_{0.069})_{\Sigma 1.00}(Fe^{2+}_{0.547}Mn_{0.453})_{\Sigma 1.00}(Fe^{2+})(Al_{0.734}Mg_{0.233}Fe^{2+}_{0.033})_{\Sigma 1.00}(PO_4)_3$ (ferrowyllieite, sample AM48D), and $Na_{0.262}(Na_{0.515}Mn_{0.451}Ca_{0.064})_{\Sigma 1.00}(Fe^{2+}_{0.514}Mn_{0.486})_{\Sigma 1.00}(Fe^{3+}_{0.559}Fe^{2+}_{0.441})(Al_{0.634}Mg_{0.229}Fe^{2+}_{0.137})_{\Sigma 1.00}(PO_4)_3$ (ferrorosemaryite, sample AM48D).

STRUCTURE REFINEMENTS OF WYLLIEITE AND QINGHEIITE

The crystal structures were refined in the $P2_1/n$ space group, which was confirmed from systematic absences, starting from the atomic coordinates of rosemaryite (Hatert *et al.* 2006). Cation occupancies were refined to obtain better agreement with the chemical compositions of wyllieite and qingheiite (Table 1). For simplicity, Ca and K, which are present in very low amounts, were not taken into account in the crystal structure refinement. Finally, the relative occupancies of Fe^{3+} and Al (or Mg) at the M(2a) and M(2b) sites, of Mn^{2+} and vacancies (or Na) at the X(1a) and M(1) sites, and of Na and vacancies at the X(2) and X(1b) sites, were refined. The refinements were completed using anisotropic displacement parameters for all atoms. The final conventional R_1 factors are 0.0272 (wyllieite from Buranga), 0.0353 (wyllieite from Malpensata), and 0.0246 (qingheiite) (Table 2).

Final positional and equivalent displacement parameters are given in Table 3, and selected bond distances and angles in Table 4. Anisotropic displacement parameters are available from the the Depository of Unpublished Data on the MAC website (document wyllieite CM54_4_10.3749/canmin.1600033). The basic structural features are identical to those of the other members of the wyllieite group (Moore & Molin-Case 1974, Zhesheng *et al.* 1983, Yakubovich *et al.* 2005, Hatert *et al.* 2005, 2006, 2010). The structure consists of kinked chains of edge-sharing octahedra stacked parallel to {101}. These chains are made up of a succession of M(2a)–M(2b) octahedral pairs, linked by slightly larger M(1) octahedra (Fig. 3). Equivalent chains are connected in the **b** direction by the P(1), P(2a), and P(2b) phosphate tetrahedra to form sheets oriented perpendicular to [010]. These interconnected sheets produce channels parallel to **c**, channels that contain the large X sites (Fig. 3).

Detailed cationic distributions have also been established by taking into account the results of the chemical analyses and of the single-crystal structure refinements. The results given in Table 5 indicate that the refined site populations (RSP), obtained from the single-crystal structure refinements (Table 3), are in good agreement with the assigned site populations (ASP), deduced from the chemical analyses. Moreover, the refined site-scattering values (RSS) and the mean bond lengths (MBL), obtained from the structure refinements, are very close to the calculated site-scattering values (CSS) and the calculated bond lengths (CBL), respectively (Table 5). This agreement again confirms the reliability of the assigned site populations.

Finally, the bond valence tables are given in Table 6, where the bond valence sums were calculated as $s = \exp[(R_0 - R)/0.37]$, by using the R_0 values of Brown & Altermatt (1985). The bond valences for oxygen are

TABLE 3. FINAL FRACTIONAL ATOMIC COORDINATES AND EQUIVALENT DISPLACEMENT PARAMETERS (Å^2) FOR WYLLIEITE FROM BURANGA, FOR WYLLIEITE FROM MALPENSATA, AND FOR QINGHEIITE FROM SANTA ANA

	Wyllieite, Buranga				Wyllieite, Malpensata				Qingheiite, Santa Ana			
Site	*x*	*y*	*z*	U_{eq}	*x*	*y*	*z*	U_{eq}	*x*	*y*	*z*	U_{eq}
X(2)	–0.0005(1)	–0.0209(2)	0.2513(3)	0.0337(7)	–0.0009(4)	–0.0174(4)	0.2558(8)	0.037(2)	–0.00063(9)	–0.0236(1)	0.2517(2)	0.0223(5)
X(1a)	0.5	0	0	0.0163(2)	0.5	0	0	0.0206(4)	0.5	0	0	0.0129(2)
X(1b)	0.5	0	0.5	0.0243(7)	0.5	0	0.5	0.031(1)	0.5	0	0.5	0.0225(6)
M(1)	–0.00015(4)	0.26349(4)	0.26157(8)	0.011(1)	0.0009(1)	0.25980(6)	0.2668(1)	0.0164(3)	–0.00122(3)	0.26403(3)	0.26282(6)	0.0101(2)
M(2a)	0.28015(5)	–0.33493(5)	0.3561(1)	0.0085(2)	0.28124(9)	–0.33512(7)	0.3576(2)	0.0136(3)	0.28287(6)	–0.33388(5)	0.3592(1)	0.0092(2)
M(2b)	0.22742(4)	–0.14840(4)	0.63788(8)	0.0092(2)	0.22333(6)	–0.14536(5)	0.6279(1)	0.0149(2)	0.22727(4)	–0.14974(4)	0.63565(8)	0.0088(2)
P(1)	0.00615(6)	–0.28347(6)	0.2412(1)	0.0084(2)	0.0057(1)	–0.28536(9)	0.2376(2)	0.0139(3)	0.00760(5)	–0.28648(5)	0.24066(9)	0.0079(2)
P(2a)	0.23815(6)	–0.09732(6)	0.1198(1)	0.0104(2)	0.2397(1)	–0.09706(9)	0.1174(2)	0.0149(3)	0.23625(5)	–0.09880(5)	0.1172(1)	0.0087(2)
P(2b)	0.23857(6)	0.11356(6)	0.6452(1)	0.0098(2)	0.2412(1)	0.11570(9)	0.6496(2)	0.0142(3)	0.23556(5)	0.11406(5)	0.64308(9)	0.0080(2)
O(1a)	0.4498(2)	–0.2846(2)	0.5198(3)	0.0126(4)	0.4477(3)	–0.2826(2)	0.5138(5)	0.0165(7)	0.4531(2)	–0.2824(1)	0.5208(3)	0.0118(3)
O(1b)	0.4537(2)	–0.7091(2)	0.0498(3)	0.0132(4)	0.4564(3)	–0.7113(2)	0.0535(5)	0.0167(7)	0.4539(2)	–0.7121(1)	0.0509(3)	0.0109(3)
O(2a)	0.1088(2)	–0.3496(2)	0.2195(4)	0.0210(5)	0.1102(3)	–0.3493(2)	0.2172(5)	0.0203(7)	0.1107(2)	–0.3538(1)	0.2216(3)	0.0151(4)
O(2b)	0.0825(2)	–0.6308(2)	0.7394(4)	0.0181(4)	0.0817(3)	–0.6269(2)	0.7460(5)	0.0198(7)	0.0828(2)	–0.6283(1)	0.7423(3)	0.0122(4)
O(3a)	0.3193(2)	–0.3265(2)	0.0863(3)	0.0160(4)	0.3170(3)	–0.3251(2)	0.0847(5)	0.0179(7)	0.3233(2)	–0.3264(1)	0.0882(3)	0.0143(4)
O(3b)	0.3411(2)	–0.6533(2)	0.6092(3)	0.0179(4)	0.3415(3)	–0.6522(2)	0.6136(5)	0.0204(7)	0.3416(2)	–0.6546(1)	0.6123(3)	0.0119(4)
O(4a)	0.1279(2)	0.4145(2)	0.3511(3)	0.0159(4)	0.1261(3)	0.4116(2)	0.3525(5)	0.0196(7)	0.1280(2)	0.4139(1)	0.3515(3)	0.0125(4)
O(4b)	0.1225(2)	–0.4033(2)	0.7822(3)	0.0134(4)	0.1191(3)	–0.3976(2)	0.7734(5)	0.0179(7)	0.1236(2)	–0.4020(1)	0.7832(3)	0.0111(3)
O(5a)	0.2376(2)	–0.1671(2)	0.3182(3)	0.0175(4)	0.2372(3)	–0.1677(3)	0.3145(5)	0.0208(7)	0.2357(2)	–0.1672(2)	0.3151(3)	0.0168(4)
O(5b)	0.2232(2)	–0.8168(2)	0.8314(4)	0.0156(4)	0.2231(3)	–0.8139(2)	0.8339(5)	0.0172(7)	0.2194(2)	–0.8172(1)	0.8272(3)	0.0122(3)
O(6a)	0.3207(2)	–0.4875(2)	0.3813(4)	0.0218(5)	0.3137(3)	–0.4853(2)	0.3771(6)	0.0231(8)	0.3253(2)	–0.4894(2)	0.3856(3)	0.0172(4)
O(6b)	0.3292(2)	–0.4925(2)	0.8831(4)	0.0202(5)	0.3212(3)	–0.4914(2)	0.8751(6)	0.0234(8)	0.3312(2)	–0.4932(1)	0.8858(3)	0.0126(4)

TABLE 4. SELECTED BOND DISTANCES (Å) AND ANGLES (°) FOR (A) WYLLIEITE FROM BURANGA, (B) WYLLIEITE FROM MALPENSATA, AND (C) QINGHEIITE FROM SANTA ANA

	A	B	C		A	B	C
P(1)–O(2a)	1.531(2)	1.532(3)	1.530(2)	X(2)–O(6a)	2.447(3)	2.513(6)	2.412(2)
P(1)–O(1b)	1.531(2)	1.526(3)	1.536(2)	X(2)–O(6b)	2.412(3)	2.465(6)	2.397(2)
P(1)–O(2b)	1.544(2)	1.546(3)	1.546(2)	X(2)–O(6b)'	2.513(3)	2.547(6)	2.492(2)
P(1)–O(1a)	1.545(2)	1.553(3)	1.549(2)	X(2)–O(1b)	2.612(3)	2.651(6)	2.616(2)
Mean	1.538	1.539	1.540	X(2)–O(6a)'	2.651(3)	2.737(6)	2.613(2)
				X(2)–O(3b)	2.771(3)	2.721(5)	2.801(2)
O(2a)–P(1)–O(1b)	115.6(1)	115.4(2)	116.22(9)	X(2)–O(1a)	2.771(3)	2.854(6)	2.768(2)
O(2a)–P(1)–O(2b)	103.8(1)	103.9(2)	103.5(1)	X(2)–O(3a)	3.122(3)	3.120(6)	3.119(2)
O(2a)–P(1)–O(1a)	105.8(1)	105.9(2)	106.0(1)	Mean*	2.662	2.641	2.652
O(1b)–P(1)–O(2b)	108.9(1)	109.3(2)	108.40(9)				
O(1b)–P(1)–O(1a)	109.3(1)	109.4(2)	109.0(1)	X(1a)–O(4b) × 2	2.159(2)	2.152(3)	2.179(2)
O(2b)–P(1)–O(1a)	113.6(1)	112.9(2)	113.92(9)	X(1a)–O(2b) × 2	2.172(2)	2.152(3)	2.163(2)
Mean	109.50	109.47	109.51	X(1a)–O(4a) × 2	2.364(2)	2.357(3)	2.362(2)
				Mean	2.232	2.220	2.235
P(2a)–O(6a)	1.536(2)	1.536(3)	1.542(2)				
P(2a)–O(4a)	1.541(2)	1.542(3)	1.548(2)	X(1b)–O(2a) × 2	2.377(2)	2.377(3)	2.350(2)
P(2a)–O(5a)	1.541(2)	1.544(3)	1.535(2)	X(1b)–O(4a) × 2	2.381(2)	2.393(3)	2.394(2)
P(2a)–O(3b)	1.543(2)	1.548(3)	1.545(2)	X(1b)–O(4b) × 2	2.690(2)	2.731(3)	2.700(2)
Mean	1.540	1.543	1.543	X(1b)–O(2b) × 2	2.788(2)	2.718(3)	2.761(2)
				Mean	2.559	2.555	2.551
O(4a)–P(2a)–O(6a)	111.5(1)	111.0(2)	112.0(1)				
O(4a)–P(2a)–O(5a)	108.3(1)	108.1(2)	108.1(1)	M(1)–O(1a)	2.207(2)	2.186(3)	2.205(2)
O(4a)–P(2a)–O(3b)	110.8(1)	111.1(2)	110.41(9)	M(1)–O(4b)	2.214(2)	2.182(3)	2.189(2)
O(6a)–P(2a)–O(5a)	110.2(1)	110.2(2)	109.6(1)	M(1)–O(1b)	2.240(2)	2.193(3)	2.227(2)
O(6a)–P(2a)–O(3b)	107.3(1)	108.6(2)	107.0(1)	M(1)–O(3b)	2.212(2)	2.200(3)	2.186(2)
O(5a)–P(2a)–O(3b)	108.6(1)	107.9(2)	109.7(1)	M(1)–O(3a)	2.265(2)	2.248(3)	2.230(2)
Mean	109.45	109.48	109.47	M(1)–O(4a)	2.339(2)	2.329(3)	2.331(2)
				Mean	2.246	2.223	2.228
P(2b)–O(6b)	1.519(2)	1.502(3)	1.524(2)				
P(2b)–O(5b)	1.546(2)	1.552(3)	1.537(2)	M(2a)–O(2a)	1.872(2)	1.874(3)	1.878(2)
P(2b)–O(4b)	1.541(2)	1.545(3)	1.551(2)	M(2a)–O(6a)	1.948(2)	1.899(3)	1.989(2)
P(2b)–O(3a)	1.543(2)	1.548(3)	1.547(2)	M(2a)–O(1a)	1.959(2)	1.936(3)	1.958(2)
Mean	1.537	1.537	1.540	M(2a)–O(3a)	1.972(2)	1.963(3)	1.994(2)
				M(2a)–O(5b)	2.032(2)	2.008(3)	2.041(2)
O(6b)–P(2b)–O(4b)	111.9(1)	111.4(2)	111.4(1)	M(2a)–O(5a)	2.139(2)	2.135(3)	2.137(2)
O(6b)–P(2b)–O(3a)	107.5(1)	108.3(2)	107.3(1)	Mean	1.987	1.969	2.000
O(6b)–P(2b)–O(5b)	110.5(1)	111.0(2)	110.9(1)				
O(4b)–P(2b)–O(3a)	110.6(1)	110.6(2)	110.8(1)	M(2b)–O(6b)	2.040(2)	1.984(3)	2.054(2)
O(4b)–P(2b)–O(5b)	107.5(1)	107.1(2)	107.43(9)	M(2b)–O(5a)	2.114(2)	2.093(3)	2.119(2)
O(3a)–P(2b)–O(5b)	108.7(1)	108.4(2)	109.0(1)	M(2b)–O(3b)	2.098(2)	2.097(3)	2.100(2)
Mean	109.45	109.47	109.47	M(2b)–O(1b)	2.131(2)	2.139(3)	2.129(2)
				M(2b)–O(2b)	2.085(2)	2.144(3)	2.076(2)
				M(2b)–O(5b)	2.163(2)	2.173(3)	2.163(2)
				Mean	2.105	2.105	2.107

* The long M(2)–O(3[a]) bond distance has not been taken into account for the average bond distance calculation.

close to the theoretical value of 2.00, and the bond valences for phosphorus are very close to the theoretical value of 5.00 (Table 6). For all the cationic sites, a good correspondence between the theoretical and the calculated valency values is observed.

Infrared Spectroscopy

The infrared spectra of the wyllieite-type phosphate minerals exhibit a complexity which is related both to the low symmetry and to the large unit-cell of the

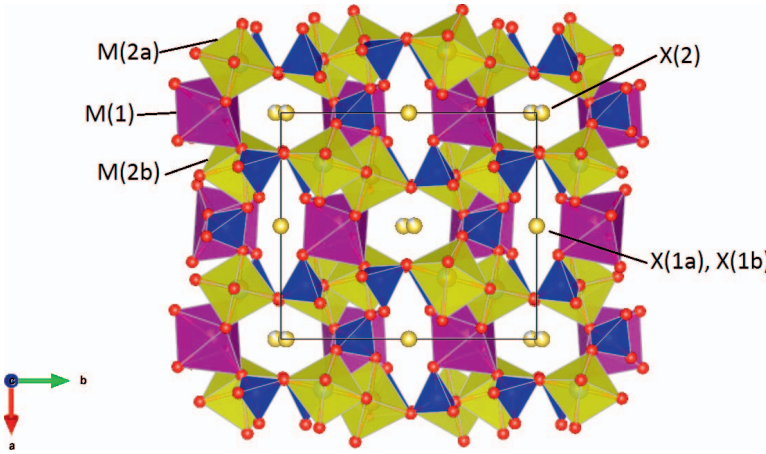

FIG. 3. The crystal structure of wyllieite from Buranga. The chains are composed of the M(1), M(2a), and M(2b) octahedra, whereas the X(1a), X(1b), and X(2) sites occur in the channels of the structure.

TABLE 5. REFINED SITE POPULATIONS (RSP, *APFU*), REFINED SITE-SCATTERING VALUES (RSS, *EPFU*), MEAN BOND-LENGTHS (MBL, Å), ASSIGNED SITE POPULATIONS (ASP, *APFU*), CALCULATED SITE-SCATTERING VALUES (CSS, *EPFU*), AND CALCULATED BOND LENGTHS (CBL, Å) FOR WYLLIEITE FROM BURANGA, FOR WYLLIEITE FROM MALPENSATA, AND FOR QINGHEIITE FROM SANTA ANA

	Results of the structure determination			Results of the chemical analysis		
Site	RSP	RSS	MBL	ASP	CSS	CBL*
			Wyllieite, Buranga			
X(2)	0.834(8) Na	9.2	2.597**	1.000 Na^{+}	11.0	2.600
X(1a)	0.989(4) Mn	24.7	2.232	1.000 Mn^{2+}	25.0	2.230
X(1b)	0.970(9) Na	10.7	2.559	1.000 Na^{+}	11.0	2.600
M(1)	0.84(1) Mn + 0.16(2) Na	22.8	2.246	0.750 Mn^{2+} + 0.200 Na^{+} + 0.050 Ca^{2+}	22.0	2.277
M(2a)	0.73(2) Al + 0.27(1) Fe	16.5	1.987	0.700 Al^{3+} + 0.250 Fe^{2+} + 0.050 Mn^{2+}	16.9	2.011
M(2b)	0.71(1) Fe + 0.29(2) Al	22.2	2.105	0.550 Fe^{2+} + 0.200 Fe^{3+} + 0.200 Mg^{2+} + 0.050 Al^{3+}	22.6	2.129
			Wyllieite, Malpensata			
X(2)	0.95(1) Na	10.5	2.641**	0.950 Na^{+}	10.5	2.600
X(1a)	0.99(2) Mn + 0.01(4) Na	24.8	2.220	0.950 Mn^{2+} + 0.050 Na^{+}	24.3	2.240
X(1b)	0.91(1) Na	10.0	2.555	0.960 Na^{+}	10.6	2.553
M(1)	0.94(1) Mn + 0.06(2) Na	24.1	2.223	0.656 Mn^{2+} + 0.278 Fe^{2+} + 0.066 Ca^{2+}	24.9	2.227
M(2a)	0.64(2) Al + 0.36(1) Fe	17.7	1.969	0.610 Al^{3+} + 0.390 Fe^{2+}	18.1	2.031
M(2b)	0.90(1) Fe + 0.10(2) Mg	24.6	2.105	0.844 Fe^{2+} + 0.048 Fe^{3+} + 0.028 Mg^{2+} + 0.080 Al^{3+}	24.6	2.152
			Qingheiite, Santa Ana			
X(2)	0.983(7) Na	10.8	2.586**	0.951 Na^{+} + 0.049 Ca^{2+}	11.4	2.597
X(1a)	0.994(4) Mn	24.9	2.235	1.000 Mn^{2+}	25.0	2.230
X(1b)	0.990(9) Na	10.9	2.551	1.000 Na^{+}	11.0	2.600
M(1)	0.976(3) Mn	24.4	2.228	0.926 Mn^{2+} + 0.074 Fe^{3+}	25.1	2.216
M(2a)	0.873(4) Al + 0.127(4) Fe	14.7	2.000	0.473 Al^{3+} + 0.343 Mg^{2+} + 0.184 Fe^{3+}	15.0	2.019
M(2b)	0.528(4) Mg + 0.472(4) Fe	18.6	2.107	0.600 Mg^{2+} + 0.400 Fe^{2+}	17.6	2.144

* The CBL values have been calculated from the ASP with the effective ionic radii of Shannon (1976), assuming a full occupancy of the crystallographic sites. ** The very long X(2)–O(3a) bonds were not taken into account for the calculation of MBL.

TABLE 6. BOND-VALENCE TABLE (*vu*) FOR WYLLIEITE FROM BURANGA, FOR WYLLIEITE FROM MALPENSATA, AND FOR QINGHEIITE FROM SANTA ANA

				Wyllieite, Buranga						
	X(2)	X(1a)	X(1b)	M(1)	M(2a)	M(2b)	P(1)	P(2a)	P(2b)	Σ
O(1a)	0.073			0.334	0.469		1.215			2.09
O(1b)	0.112			0.306		0.335	1.262			2.02
O(2a)			0.212 *		0.593		1.262			2.07
O(2b)		0.356 *	0.070 *			0.380	1.218			2.02
O(3a)				0.286	0.453				1.221	1.96
O(3b)	0.073			0.330		0.367		1.221		1.99
O(4a)		0.212 *	0.210 *	0.234				1.228		1.88
O(4b)		0.369 *	0.091 *	0.328					1.228	2.02
O(5a)					0.288	0.351		1.228		1.87
O(5b)					0.385	0.307			1.212	1.90
O(6a)	0.175				0.483			1.245		}
O(6a)'	0.101									} 2.00
O(6b)	0.193					0.429			1.303	}
O(6b)'	0.147									} 2.07
$S_{calc.}$	0.88	1.87	1.17	1.82	2.67	2.17	4.96	4.92	4.96	
$S_{theor.}$	1.00	2.00	1.00	1.80	2.70	2.25	5.00	5.00	5.00	
				Wyllieite, Malpensata						
	X(2)	X(1a)	X(1b)	M(1)	M(2a)	M(2b)	P(1)	P(2a)	P(2b)	Σ
O(1a)	0.058			0.339	0.505		1.189			2.09
O(1b)	0.101			0.333		0.329	1.279			2.04
O(2a)			0.174 *		0.597		1.258			2.03
O(2b)		0.377 *	0.069 *			0.324	1.212			1.98
O(3a)				0.287	0.470				1.205	1.96
O(3b)	0.084			0.327		0.368		1.205		1.98
O(4a)		0.216 *	0.167 *	0.231				1.225		1.84
O(4b)		0.377 *	0.067 *	0.433					1.215	2.00
O(5a)					0.295	0.372		1.218		1.89
O(5b)					0.416	0.300			1.192	1.91
O(6a)	0.147				0.558			1.245		}
O(6a)'	0.080									} 2.03
O(6b)	0.167					0.500			1.365	}
O(6b)'	0.134									} 2.17
$S_{calc.}$	0.77	1.94	0.96	1.86	2.84	2.19	4.94	4.89	4.98	
$S_{theor.}$	0.95	1.95	0.96	2.00	2.61	2.13	5.00	5.00	5.00	
				Qingheiite, Santa Ana						
	X(2)	X(1a)	X(1b)	M(1)	M(2a)	M(2b)	P(1)	P(2a)	P(2b)	Σ
O(1a)	0.075			0.324	0.479		1.202			2.08
O(1b)	0.114			0.305		0.322	1.245			1.99
O(2a)			0.228 *		0.594		1.265			2.09
O(2b)		0.366 *	0.075 *			0.371	1.215			2.03
O(3a)				0.303	0.434				1.208	1.95
O(3b)	0.069			0.341		0.348		1.215		1.97
O(4a)		0.213 *	0.202 *	0.230				1.205		1.85
O(4b)		0.349 *	0.089 *	0.338					1.195	1.97
O(5a)					0.295	0.331		1.248		1.87
O(5b)					0.382	0.293			1.241	1.92
O(6a)	0.197				0.440			1.225		}
O(6a)'	0.114									} 1.98
O(6b)	0.205					0.394			1.286	}
O(6b)'	0.159									} 2.04
$S_{calc.}$	0.93	1.86	1.19	1.84	2.62	2.06	4.93	4.89	4.93	
$S_{theor.}$	1.05	2.00	1.00	2.07	2.66	2.00	5.00	5.00	5.00	

Note: The bond valences were calculated from the bond lengths given in Table 4, and from the assigned site populations of Table 5, with the parameters of Brown & Altermatt (1985). * Bond valences were multiplied by two, for the calculation of the valence on the X(1a) and X(1b) crystallographic sites. The very long X(2)–O(3a) distances were not taken into account in the calculations.

wyllieite structure; for this reason, it is difficult to assign all the individual absorption bands. Nevertheless, the similarities between the spectra of wyllieite and qingheiite (Fig. 1) and those of ferrorosemaryite and rosemaryite permits the assignments proposed by Hatert *et al*. (2005, 2006) to be used for the samples investigated herein. According to these authors, the stretching vibrational modes of the PO_4 tetrahedra occur in the 1200–900 cm^{-1} region, whereas both the PO_4 bending vibrations and the AlO_6 and FeO_6 stretching vibrational modes contribute to the absorption between *ca*. 400 and 650 cm^{-1}. At lower frequencies is the domain of lattice vibrations.

It is important to note a large absorption band, localized around 3300–3400 cm^{-1} (Fig. 1), which is related to the O–H stretching vibrational mode (Farmer 1974). The presence of protons in natural alluaudites was suspected by Fransolet *et al*. (1994) on the basis of wet chemical analyses, and the synthetic protonated alluaudite-type compounds $M^{+}M^{2+}{}_3(PO_4)(HPO_4)_2$ (M^{+} = Na, Ag; M^{2+} = Mn, Co) were synthesized by Lii & Shih (1994), Leroux *et al*. (1995a,b), and Guesmi & Driss (2002). The infrared spectra of wyllieite and qingheiite do not show any supplementary absorption band around 1600 cm^{-1}, related to the bending vibrational mode of H_2O, thus demonstrating the absence of molecular water in the channels of the structure. Consequently, the bands at 3433 and 3318 cm^{-1} could be attributed to the stretching vibrations of OH^{-} groups localized at the apex of $HPO_4{}^{2-}$ tetrahedra, as previously observed by Hatert *et al*. (2005) in ferrorosemaryite.

Discussion

Crystal chemistry of wyllieite-type phosphate minerals

The crystal structure of wyllieite-group minerals was first solved by Moore & Molin-Case (1974) for a sample of ferrowyllieite; then Zhesheng *et al*. (1983) reported the structure of qingheiite. A careful examination of the atomic coordinates in Hatert *et al*. (2006) has shown, however, that the M(2a)-M(2b) and X(1a)-X(1b) pairs of crystallographic sites, which result from a splitting of the M(2) and X(1) sites of the alluaudite structure, are inverted in qingheiite. More recently, four structure refinements were reported for the new mineral species ferrorosemaryite (Hatert *et al*. 2005) and qingheiite-(Fe^{2+}) (Hatert *et al*. 2010), as well as for rosemaryite from Buranga (Hatert *et al*. 2006) and the synthetic compound $Na_{1.265}Mn^{2+}{}_{2.690}Mn^{3+}{}_{0.785}(PO_4)_3$ (Yakubovich *et al*. 2005). These papers helped us to better understand the crystal chemistry of the wyllieite-type phosphates.

The three samples, investigated herein, are weakly oxidized, compared to ferrorosemaryite and rosemaryite, and contain a low number of vacancies, since the oxidation mechanism of wyllieite-type phosphates is $Na^{+} + Fe^{2+} = \square + Fe^{3+}$ (Fransolet 1995). For this reason, all crystallographic sites were observed, including the X(2) site which is vacant in ferrorosemaryite (Hatert *et al*. 2005). Bond distances and angles (Table 4) indicate that all of the crystallographic sites have topologies similar to those described by Hatert *et al*. (2006) for the sites in rosemaryite. The anion coordination of the X(2) site corresponds to a [7 + 1]-coordinated distorted gable disphenoid, similar to the A(2)' site of the alluaudite structure (Hatert *et al*. 2000, Hatert 2002, 2004, 2008), while that of the X(1a) site is a very distorted octahedron, and that of the X(1b) site is a distorted cube similar to the A(1) site in the alluaudites. The M(2a), M(2b), and M(1) sites are coordinated by fairly regular octahedra (Table 4).

Cationic distributions (Table 5) show that the X(2) and X(1b) sites are nearly fully occupied by Na, whereas X(1a) is nearly fully occupied by Mn. At the M(1) site, Mn is dominant, associated with smaller amounts of Na, Ca, Fe^{2+}, or Fe^{3+}. As previously noted by Hatert *et al*. (2005, 2006, 2010) for ferrorosemaryite, rosemaryite, and qingheiite-(Fe^{2+}), the distributions of Fe, Mg, and Al between the M(2a) and M(2b) crystallographic sites are different from that occurring in ferrowyllieite. Re-examination of the atomic coordinates and bond-length distortion coefficients (see below) indicate, however, that the M(2a)-M(2b) and X(1a)-X(1b) pairs of crystallographic sites are inverted in ferrowyllieite, qingheiite, and in the compound synthesized by Yakubovich *et al*. (2005), compared to the coordinates published by Hatert *et al*. (2005, 2006, 2010), and to those in the present paper. In the following discussion, we will use the site nomenclature of rosemaryite (Hatert *et al*. 2006).

The M(2a) site of the samples investigated herein, with average M(2a)–O bond lengths from 1.969 to 2.000 Å, is smaller than the M(2b) site, with average M(2b)–O bond lengths from 2.105 to 2.107 Å (Table 4). For this reason, Al, with an effective ionic radius (*e.i.r.*) of 0.535 Å (Shannon 1976), preferentially occurs at M(2a), while Fe^{2+} (*e.i.r.* 0.780 Å) and Mg (*e.i.r.* 0.720 Å) preferentially occur at M(2b). In conclusion, the M(2a) site of the wyllieite-type phosphates is dominantly occupied by Al; M(2b) by Fe^{2+}, Fe^{3+} or Mg; M(1) by Mn or Fe^{2+}; X(1a) by Mn; and X(1b) and X(2) by Na and vacancies.

Variations of M–O bond lengths and polyhedral distortion

In the wyllieite structure, cations occurring at X(2), X(1a), and X(1b) are located in the channels of the

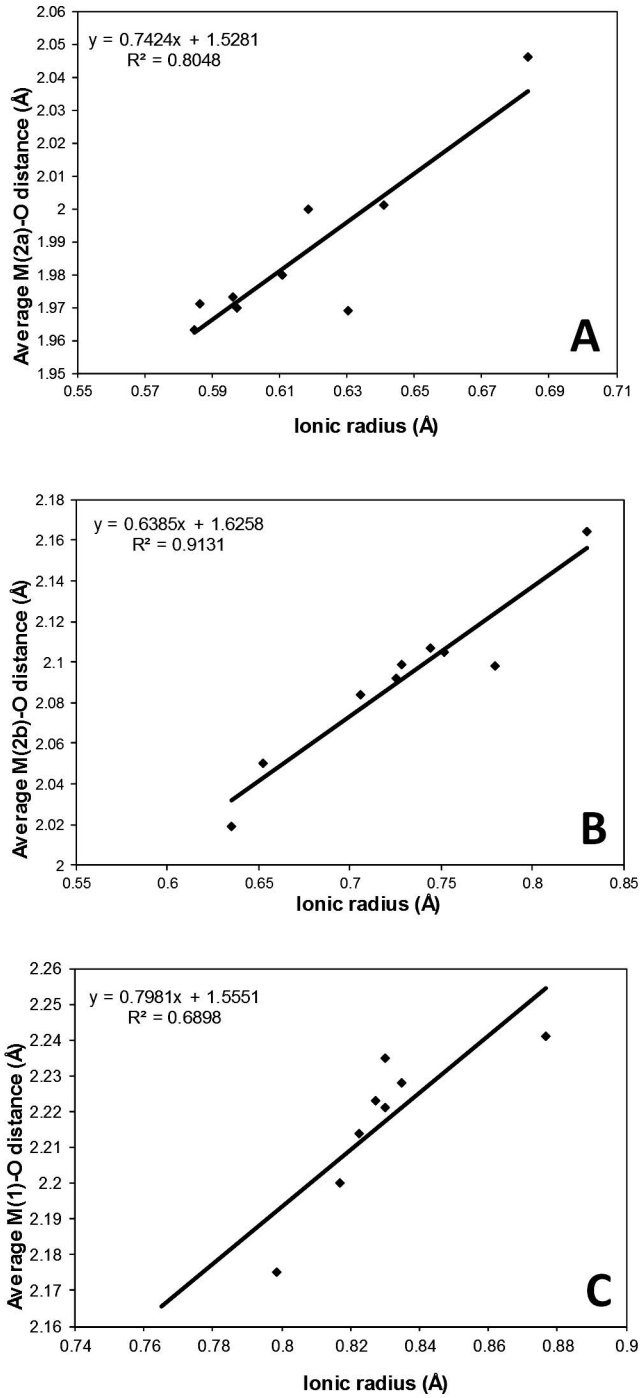

FIG. 4. Correlations between the M(2a)–O (a), M(2b)–O (b), and M(1)–O (c) bond distances and the mean ionic radius of the cations occurring at these sites. Data from Moore & Molin-Case (1974), Zhesheng *et al*. (1983), Yakubovich *et al*. (2005), and Hatert *et al*. (2005, 2006, 2010).

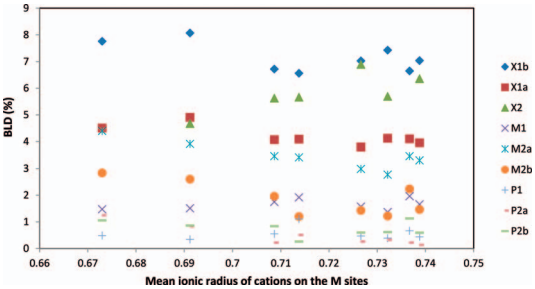

FIG. 5. Correlations between the bond length distortion coefficients for the crystallographic sites of the wyllieite-type phosphates and the mean ionic radius of cations occurring at the M sites. Distortion coefficients calculated from the structural data of Moore & Molin-Case (1974), Zhesheng *et al*. (1983), Yakubovich *et al*. (2005), and Hatert *et al*. (2005, 2006, 2010).

structure (Fig. 3); consequently, they can be considered as extra-framework cations. For this reason, it is difficult to correlate the X–O distances with the effective ionic radii of these cations, due to the presence of significant amounts of vacancies. Concerning the M sites, good correlations are observed between the M–O distances and the average effective ionic radii of the cations occurring at these sites (Fig. 4), thus confirming the cationic distributions at these sites.

Bond-length distortion coefficients (BLD) were also calculated for the crystallographic sites of the wyllieite-type phosphates from the bond distances given in Table 4, using a method from Renner & Lehmann (1986) modified by Hatert *et al*. (2004) (Table 6). As shown in Figure 5, these coefficients generally decrease when the average ionic radius of the cations occurring at the M sites increases; only the X(2) and M(1) polyhedra show the inverse behavior. The most distorted anion coordination in the wyllieite-type structure is around X(1b) (BLD ~ 6–8%), with its topology of a distorted cube, followed by X(2) (BLD ~ 4–7%), with its topology of a distorted gable disphenoid (Table 7, Fig. 5). Two groups can be distinguished among the four octahedral coordinations: highly distorted around the X(1a) position (BLD ~ 4–5%) and the M(2a) (BLD 3–4.5%) site, and weakly distorted around the M(1) (BLD ~ 1–2%) and M(2b) (BLD ~ 1–3%) sites. The tetrahedra show very low bond length distortion coefficients, generally below 1%.

A comparison with the bond-length distortion coefficients calculated by Hatert *et al*. (2004) for natural and synthetic alluaudite-type phosphates indicates very close values of BLD for the M(1) sites in both structure types (alluaudites 1.22–2.05%; wyllieites 1.37–1.96%). The bond-length distortion coefficients for the M(2) site in the alluaudites range from 2.79 to 4.97%, values which are very close to those observed for the M(2a) site of the wyllieite structure (Table 7, Fig. 5); this indicates that the morphology of the coordinations around both crystallographic sites is very similar.

Variations of unit-cell parameters

As mentioned above, the cations occurring at the X sites can be considered as extra-framework cations. Due to the presence of significant amounts of vacancies at these sites, we attempted to correlate

TABLE 7. BOND LENGTH DISTORTION COEFFICIENTS (BLD*) FOR THE CRYSTALLOGRAPHIC SITES OF WYLLIEITE-GROUP MINERALS

Ref.	[1]	[2]	[3]	[4]	[5]	[6]	[7]	[8]
X(2)	5.66	5.69	-	4.67	5.63	6.36	5.81	6.89
X(1a)	4.09	4.12	4.50	4.91	4.07	3.95	4.10	3.80
X(1b)	6.56	7.43	7.76	8.07	6.72	7.03	6.64	7.03
M(1)	1.92	1.37	1.48	1.51	1.75	1.66	1.96	1.57
M(2a)	3.42	2.77	4.40	3.91	3.46	3.30	3.46	2.98
M(2b)	1.20	1.22	2.83	2.60	1.96	1.46	2.23	1.43
P(1)	1.11	0.39	0.49	0.34	0.55	0.44	0.67	0.47
P(2a)	0.51	0.33	1.25	0.83	0.23	0.14	0.23	0.26
P(2b)	0.26	0.62	1.06	0.86	0.84	0.59	1.13	0.60

Note: [1] Ferrowyllieite, Moore & Molin-Case (1974); [2] Qingheiite, Zhesheng *et al*. (1983); [3] Ferrorosemaryite, Hatert *et al*. (2005); [4] Rosemaryite, Hatert *et al*. (2006); [5] Qingheiite-(Fe^{2+}), Hatert *et al*. (2010); [6] Wyllieite, Buranga (this work); [7] Wyllieite, Malpensata (this work); [8] Qingheiite, Santa Ana (this work).

* BLD $= \frac{100}{n} \times \sum_{i=1}^{n} \frac{di - dm}{dm}$, where n is the number of bonds, dm the mean bond length, and di the individual bond lengths.

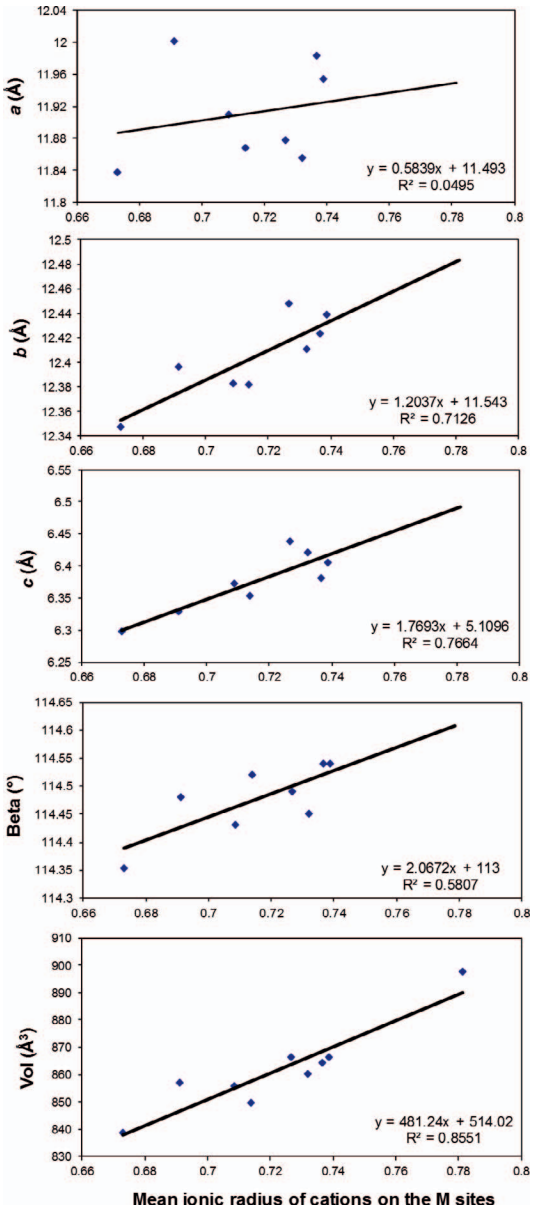

FIG. 6. Correlations between the unit-cell parameters of the wyllieite-type phosphates and the mean ionic radius of cations occurring at the M sites. Data from Moore & Molin-Case (1974), Zhesheng *et al*. (1983), Yakubovich *et al*. (2005), and Hatert *et al*. (2005, 2006, 2010).

the unit-cell parameters of wyllieite-type phosphates with the mean ionic radius of the cations occurring at the framework M crystallographic sites. As shown in Figure 6, good correlations are observed for the *b* and *c* parameters, as well as for the unit-cell volume; the

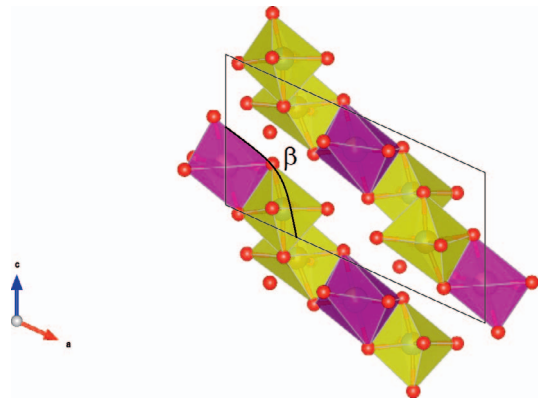

FIG. 7. Projection of the octahedral M chains of the wyllieite structure, showing the relationship between the [M(1)–M(2a)] + [M(1)–M(2b)] bond length and the β unit-cell angle.

corresponding equations can consequently be used to estimate the mean ionic radius of M cations in wyllieite-type compounds.

Hatert (2008) established a correlation between the M(1)–M(2) bond length in alluaudite-type phosphates and the β angle; indeed, the octahedral chains of the structure are parallel to {101}, and variations of their elongation consequently modify the β unit-cell angle. A similar behavior is expected in the wyllieite-type phosphates, due to the same orientation of the octahedral M chains (Fig. 7). As shown in Figure 8, a fairly good correlation exists between the β angle and the [M(1)–M(2a)] + [M(1)–M(2b)] bond length, indicating that the hypothesis formulated by Hatert (2008) is also valid for the wyllieite-type phosphates.

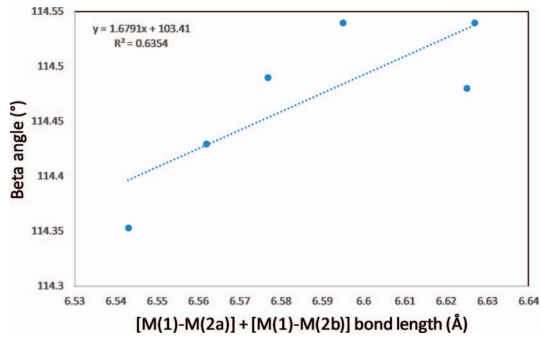

FIG. 8. Correlations between the [M(1)–M(2a)] + [M(1)–M(2b)] bond distance of wyllieite-type phosphates and the β unit-cell angle. Data from Hatert *et al*. (2005, 2006, 2010).

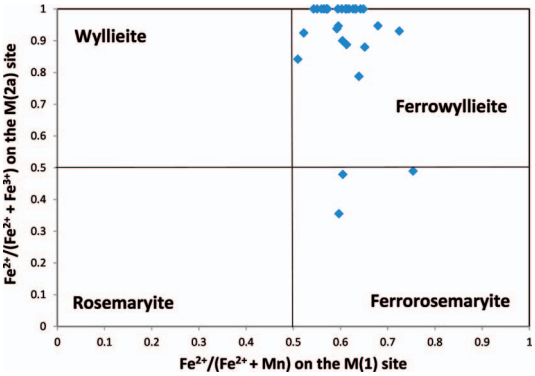

FIG. 9. Diagram representing the members of the wyllieite group, from which were reported the electron-microprobe compositions of samples from the Albères Massif.

The oxidation of ferrowyllieite to ferrorosemaryite

Petrographic observations of phosphates from the Albères Massif show that ferrowyllieite is transformed to ferrorosemaryite along fractures and on the rims of the crystals (Fig. 2b). The electron-microprobe analyses of these minerals (Table 1) are reported on the diagram established by Hatert *et al*. (2005) to distinguish the phosphates of the wyllieite group (Fig. 9). As shown on this diagram, most compositions correspond to ferrowyllieite, but some grains contain significant amounts of Fe^{3+} at the M(2a) site, indicating an oxidation towards ferrorosemaryite. Three point analyses correspond to this mineral (Fig. 9); this is the second world occurrence for the species.

The oxidation mechanism, responsible for the oxidation of ferrowyllieite to ferrorosemaryite, is $Na^{+} + Fe^{2+} = \square + Fe^{3+}$. This mechanism was described by Fontan *et al*. (1994), Fransolet (1995), and Hatert *et al*. (2005) for the wyllieite–rosemaryite series, and by Fransolet *et al*. (2004) for the alluaudite-type phosphates. However, the oxidation mechanism is identified here for the first time in the ferrowyllieite–ferrorosemaryite series. As shown in Figure 10, an excellent correlation exists between ($Na + Fe^{2+}$) and ($\square + Fe^{3+}$), with a slope very close to –1, thus confirming the oxidation mechanism mentioned above.

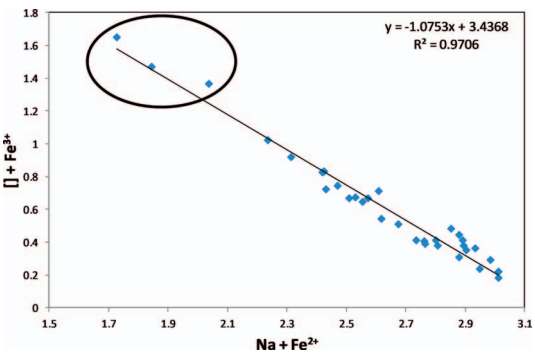

FIG. 10. Correlation between ($Na + Fe^{2+}$) and ($\square + Fe^{3+}$) in ferrowyllieite and ferrorosemaryite samples from the Albères Massif. The elliptic zone contains the three point analyses of ferrorosemaryite.

ACKNOWLEDGMENTS

This paper is dedicated to Skip Simmons and Karen L. Webber, for their outstanding contribution to the petrography and mineralogy of granitic pegmatites. Many thanks are due to J.-C. Melgarejo and F. Fontan (†), who provided us with the phosphate samples from the Albères Massif, as well as to Nicola Rotiroti and an anonymous reviewer for their constructive comments.

REFERENCES

BROWN, I.D. & ALTERMATT, D. (1985) Bond-valence parameters obtained from a systematic analysis of the inorganic crystal structure database. *Acta Crystallographica* **B41**, 244–247.

ČERNÝ, P. (1991) Rare-element granitic pegmatites. Part I: Anatomy and internal evolution of pegmatite deposits. *Geosciences Canada* **18(2)**, 49–67.

ČERNÝ, P. & ERCIT, T.S. (2005) The classification of granitic pegmatites revisited. *Canadian Mineralogist* **40**, 2005–2026.

FARMER, V.C. (1974) The infrared spectra of minerals. *Mineralogical Society Monographs* **4**, 539 pp.

FONTAN, F., RODA, E., PESQUERA, A., & VELASCO, F. (1994) The phosphate mineral association of Fregeneda pegmatites (Salamanca, Spain). Abstracts Book, 16th General Meeting International Mineralogical Association, Pisa, Italy, 122 pp.

FRANSOLET, A.-M. (1975) *Etude minéralogique et pétrologique des phosphates de pegmatites granitiques*. Unpublished Ph.D. Thesis, University of Liège, Liège, Belgium, 333 pp.

FRANSOLET, A.-M. (1995) Wyllieite et rosemaryite dans la pegmatite de Buranga, Rwanda. *European Journal of Mineralogy* **7**, 567–575.

FRANSOLET, A.-M., ANTENUCCI, D., FONTAN, F., & KELLER, P. (1994) New relevant data on the crystal chemistry, and on the genetical problem of alluaudites and wyllieites. Abstracts Book, of the 16th General Meeting International Mineralogical Association, Pisa, Italy, 125–126.

FRANSOLET, A.-M., HATERT, F., & FONTAN, F. (2004) Petrographic evidence for primary hagendorfite in an unusual assemblage of phosphate minerals, Kibingo granitic pegmatite, Rwanda. *Canadian Mineralogist* **42**, 697–704.

Galliski, M.A., Oyárzabal, J.C., Márquez-Zavalía, M.F., & Chapman, R. (2009) The association qingheiite–beusite–lithiophilite in the Santa Ana pegmatite, San Luis, Argentina. *Canadian Mineralogist* **47**, 1213–1223.

Guesmi, A. & Driss, A. (2002) $AgCo_3PO_4(HPO_4)_2$. *Acta Crystallographica* **C58**, i16–i17.

Hatert, F. (2002) *Cristallochimie et synthèse hydrothermale d'alluaudites dans le système Na–Mn–Fe–P–O: contribution au problème de la genèse de ces phosphates dans les pegmatites granitiques*. Unpublished Ph.D. Thesis, University of Liège, Liège, Belgium, 247 pp.

Hatert, F. (2004) Etude cristallochimique et synthèse hydrothermale des alluaudites: contribution nouvelle au problème génétique des phosphates de fer et de manganèse dans les pegmatites granitiques et, partant, à celui de l'évolution de ces gisements. *Mémoire de l'Académie royale des Sciences de Belgique, Classe des Sciences, Collection in-8°, 3ème série* **XXI**, 96 pp.

Hatert, F. (2008) The crystal chemistry of the divalent cation in alluaudite-type phosphates: a structural and infrared spectral study of the solid solutions $Na_{1.5}(Mn_{1-x}M^{2+}_x)_{1.5}Fe_{1.5}(PO_4)_3$ ($x = 0$ to 1, $M^{2+} = Cd^{2+}$, Zn^{2+}). *Journal of Solid State Chemistry* **181**, 1258–1272.

Hatert, F., Keller, P., Lissner, F., Antenucci, D., & Fransolet, A.-M. (2000) First experimental evidence of alluaudite-like phosphates with high Li-content: the $(Na_{1-x}Li_x)MnFe_2(PO_4)_3$ series ($x = 0$ to 1). *European Journal of Mineralogy* **12**, 847–857.

Hatert, F., Long, G.J., Hautot, D., Fransolet, A.-M., Delwiche, J., Hubin-Franskin, M.J., & Grandjean, F. (2004) A structural, magnetic, and Mössbauer spectral study of several Na-Mn-Fe-bearing alluaudites. *Physics and Chemistry of Minerals* **31**, 487–506.

Hatert, F., Lefèvre, P., Fransolet, A.-M., Spirlet, M.-R., Rebbouh, L., Fontan, F., & Keller, P. (2005) Ferrorosemaryite, $NaFe^{2+}Fe^{3+}Al(PO_4)_3$, a new phosphate mineral from the Rubindi pegmatite, Rwanda. *European Journal of Mineralogy* **17**, 749–759.

Hatert, F., Hermann, R.P., Fransolet, A.-M., Long, G.J., & Grandjean, F. (2006) A structural, infrared, and Mössbauer spectral study of rosemaryite, $NaMnFe^{3+}Al(PO_4)_3$. *European Journal of Mineralogy* **18**, 775–785.

Hatert, F., Baijot, M., Philippo, S., & Wouters, J. (2010) Qingheiite-(Fe^{2+}), $Na_2Fe^{2+}MgAl(PO_4)_3$, a new phosphate mineral from the Sebastião Cristino pegmatite, Minas Gerais, Brazil. *European Journal of Mineralogy* **22**, 459–467.

Leroux, F., Mar, A., Payen, C., Guyomard, D., Verbaere, A., & Piffard, Y. (1995a) Synthesis and structure of $NaMn_3(PO_4)(HPO_4)_2$, an unoxidized variant of the alluaudite structure type. *Journal of Solid State Chemistry* **115**, 240–246.

Leroux, F., Mar, A., Guyomard, D., & Piffard, Y. (1995b) Cation substitution in the alluaudite structure type: synthesis and structure of $AgMn_3(PO_4)(HPO_4)_2$. *Journal of Solid State Chemistry* **117**, 206–212.

Lii, K.-H. & Shih, P.-F. (1994) Hydrothermal synthesis and crystal structures of $NaCo_3(PO_4)(HPO_4)_2$ and $NaCo_3(AsO_4)(HAsO_4)_2$: synthetic modifications of the mineral alluaudite. *Inorganic Chemistry* **33**, 3028–3031.

Malló, A., Fontan, F., Melgarejo, J.-C., & Mata, J.M. (1995) The Albera zoned pegmatite field, eastern Pyrenees, France. *Mineralogy and Petrology* **55**, 103–116.

Moore, P.B. (1971) Crystal chemistry of the alluaudite structure type: Contribution to the paragenesis of pegmatite phosphate giant crystals. *American Mineralogist* **56**, 1955–1975.

Moore, P.B. & Ito, J. (1973) Wyllieite, $Na_2Fe^{2+}{}_2Al(PO_4)_3$, a new species. *Mineralogical Record* **4**, 131–136.

Moore, P.B. & Ito, J. (1979) Alluaudites, wyllieites, arrojadites: crystal chemistry and nomenclature. *Mineralogical Magazine* **43**, 227–235.

Moore, P.B. & Molin-Case, J. (1974) Contribution to pegmatite phosphate giant crystal paragenesis: II. The crystal chemistry of wyllieite, $Na_2Fe^{2+}{}_2Al(PO_4)_3$, a primary phase. *American Mineralogist* **59**, 280–290.

Oxford Diffraction (2007) *CrysAlis CCD* and CrysAlis RED, *version 1.71*. Oxford Diffraction, Oxford, England.

Renner, B. & Lehmann, G. (1986) Correlation of angular and bond length distortion in TiO_4 units in crystals. *Zeitschrift für Kristallographie* **175**, 43–59.

Shannon, R.D. (1976) Revised effective ionic radii and systematic studies of interatomic distances in halides and chalcogenides. *Acta Crystallographica* **A32**, 751–767.

Sheldrick, G.M. (1993) *SHELXL93: Program for the Refinement of Crystal Structures*. University of Göttingen, Göttingen, Germany.

Sheldrick, G.M. (2008) A short history of SHELX. *Acta Crystallographica* **A64**, 112–122.

Vignola, P., Fransolet, A.M., Guastoni, A., & Appiani, R. (2011) Le pegmatiti di Piona. Recenti studi sui filoni Malpensata, Luna e Sommafiume. *Rivista Mineralogica Italiana* **1/2011**, 30–38.

Yakubovich, O.V., Massa, W., Gavrilenko, P.G., & Dimitrova, O.V. (2005) The crystal structure of a new synthetic member in the wyllieite group: $Na_{1.265}Mn^{2+}{}_{2.690}Mn^{3+}{}_{0.785}(PO_4)_3$. *European Journal of Mineralogy* **17**, 741–747.

Zhesheng, M., Nicheng, S., & Zhizhong, P. (1983) Crystal structure of a new phosphatic mineral-quingheiite. *Scientica Sinica, série B* **XXVI(8)**, 876–884.

Received April 14, 2016. Revised manuscript accepted July 25, 2016.